CFD assessment of the effect of nanoparticles on the heat transfer properties of acetone/$ZnBr_2$ solution

Hayder I. Mohammed, Donald Giddings, Gavin S. Walker and Henry Power

Abstract

A potential novel working fluid for vapour absorption refrigeration utilising very low grade waste heat, is based on acetone and zinc bromide as the salt solution. A Computational Fluid Dynamics (CFD) model is presented of the fluid with zinc oxide nano-particles in a flat tube flow. A two phase type of model represents the zinc oxide nano-particles as a distinct fluid phase. The cases of laminar and turbulent flow are explored numerically for a wide range of acetone and nanoparticles concentrations. The velocity is varied between 1.5 - 6 ms^{-1}, representing typical heat exchanger conditions. Reynolds number depends significantly on the solution concentration. Heat transfer coefficient increases with Re, by turbulent mixing, and with the concentration of nanoparticles and of acetone by the enhanced thermal diffusivity. The shear wall stress is not affected by changing the concentration of nano-particles. The nano-fluid is demonstrated to work well for heat transfer enhancement over the base fluid; the further issue of suspension of the nano-particles in the solution is explored experimentally. The nano-fluid can be achieved by ultra-sonic excitation, with a settling time in the order of several hours. Subject to the particle suspension time being increased, this fluid combination is a good candidate for the application considered.

Keywords

Nanofluid, acetone/zinc bromide, CFD, Heat transfer, flat tube, two phase approach.

Nomenclature

Ac	Acetone	Greek letters	
c	Correction factor	ρ	Density (kg/m^3)
C_f	Skin friction	δ	Distance between centres of two particles (m)
c_p	Specific heat (J/kg.K)	μ	Viscosity (kg/m.s)
d	Diameter (m)	φ	Volume fraction
d_h	Hydraulic diameter (m)	τ_w	Wall shear stress
h	Heat transfer coefficient ($W/m^2.K$)	ν	Velocity (m/s)
K_t	Turbulence kinetic energy	ε	Rate of dissipation
k	Thermal conductivity (W/m.K)		
k_b	Boltzmann cons.		
n	Shape factor	Subscripts	
Nu	Nusselt number	*t*	Turbulence
p	Pressure (pa)	*av*	Average
Re	Reynolds number	*cl*	Centreline
T	Temperature (K)	*dr*	Drift

Ti	Turbulence intensity	*f*	Base fluid
V	Volume (m^3)	*k*	Component
V_B	Brownian velocity (m/s)	*m*	Mixture
X	Length (m)	*nf*	Nanofluid
Phi	Volume fraction	*p*	Particle

1- Introduction

With increasing demands on energy efficiency, making use of low grade waste heat using vapour absorption refrigeration systems (VARS) is receiving renewed interest; Sun et al. [1] provides an extensive review of the various working fluids for absorption refrigeration, where acetone and zinc bromide operate at the lowest boiler temperatures. These materials work with low temperature heat sources [2], much lower than most common binary fluid systems (e.g. NH_3/H_2O & H_2O/LiBr), in the order of 10s of °C above ambient. There is a large body of research focused on nanofluids, which are defined as a base fluid with particles in nanoscale (<100nm) since 'nanofluid' was first termed by Choi and Eastman [3]. It is well known that enhancement of heat transfer is possible and vehicle engine coolant heat exchangers, with either water (H_2O) or ethylene glycol (EG), in particular, have received some attention in the area.

The effect and mode of action of nanofluid on heat transfer appears to be flow situation specific. Wen and Ding [4] stated that the improvement of heat transfer of spherical Al_2O_3-water nanofluids might be caused by the particle movement due to viscosity and Brownian motion. They claimed that particle movement generates a non-uniform thermal conductivity performance which results in a higher Nusselt number. Hwang et al. [5] argued that it is caused by nano-particle migration toward the centre of the channel which generates a random velocity caused by a non-uniform viscosity. Wen and Ding [6] and Hwang et al. [5] state that most heat transfer enhancement for Al_2O_3-water nanofluids occurs in the developing region of the flow.

Ding et al. and Garg et al. [7, 8] explained the mechanism of improved heat transfer for carbon nano-tube (CNT) nanofluid by a three dimensional web of nanotubes with heat transferred within the nanotubes, which has a much higher thermal conductivity than the base fluid. Ding et al. [7] reported for carbon nano-tube (CNT) and water (0.5 wt. % of CNT) nanofluid a heat transfer enhancement of 350%. Garg et al. [8] and Lao and Liu [9] reported much lower local heat transfer coefficient enhancements for CNT nanofluids when they used a higher solid concentration.

Some researchers try to develop the nanofluid to enhance the heat transfer. In two separate studies [10, 11] Takabi and his groups numerically studies the effect of the hybrid nanofluid (two or more types of nanoparticle in form of mixture or composite suspend in a basefluid [12]) which presented by Al_2O_3 – Cu / H_2O on the heat transfer in the uniform heated circular tube for turbulent and laminar regimes. They found that the heat transfer improved for the hybrid nanofluid more than the pure water or Al_2O_3 / H_2O. in the laminar case, which studied in [10] the Nu which present the heat transfer enhanced by 7.2 % for the hybrid nanofluid compared with the base fluid. However, in [11] which involved with the turbulent flow with the wide range of Re (10^4 – 10^5) and volume fraction of the nanoparticles (0 – 2 %) they confirm that the maximum improvement in the Nu reaches to 32.02 % in the Hybrid nanofluid compared with the pure fluid.

Some researchers [13-15] reported that heat transfer in nanofluids can be modelled using classical correlations (based on Maxwell) for single-phase fluids with adjustment for properties with the nano-particles. Others stated that the heat transfer behaviour obeys a two phase model with variation due to concentration of nano-particles varying in the flow. There is a debate in the literature about which analysis provides a better prediction.

Utomo et al. [16] investigated the heat transfer coefficient arising from alumina, titania and CNT nanofluids. They found that the addition of nanoparticles to liquids enhances the heat transfer coefficients by no more than 10% at a constant turbulent velocity. They state nanofluids behaved as homogenous mixtures with experimental Nusselt numbers following classical relations developed for the single-phase approach, modified for the mean nano-particle concentration, being accurate to within ±10%; this uncertainty is explained by movement of nanoparticles due to Brownian motion and viscosity gradient due to concentration, with non-uniform shear rate having insignificant effect on heat transfer. Similar uncertainty was found for metal oxide nanofluids [17] and for CNT nano-fluids [9].

Pantzali et al. [18] investigated a nanofluid of 4 Vol. % CuO in H_2O numerically and experimentally using a laminar flow on a plate heat exchanger. They found that the flow rate of the nanofluid required for a particular heat transfer rate was lower than the base fluid. Jafari and his group [19] numerically investigated the heat transfer enhancement for the laminar and mix convection in a cavity used with Cu / H_2O nanofluid. They confirmed that the Grashof and Reynold Numbers have a great impact on improving the Nu and they stated that with increasing in the nanoparticles, the heat transfer is enhanced and it becomes more effective with a high Grashof numbers.

A two dimensional single phase CFD model was numerically studied by Demir et al [20] using Al_2O_3 and TiO_2 in water nanofluid in a horizontal pipe heat exchanger. They found that the heat transfer increased with the concentration of nanoparticles. Goktepe et al. [21] studied the single and the two phase models for nanofluid inside a uniformly heated tube. They found that the convective heat transfer coefficient is more correctly predicted with a two phase model than the single phase.

Amoura et al. [22] studied the heat transfer for three different types of nanofluid (H_2O/CuO, H_2O/Al_2O_3 and H_2O/TiO_2) in horizontal tubes in 2D with different Reynolds number up to 600 and different volume fraction of nanoparticles (0, 0.01, 0.02, 0.03 and 0.1) using a single phase technique. They found that the Nusselt number of nanofluids is larger than that of the base fluid and that the Pressure loss coefficient drops by increasing Reynolds number for all types of nanofluids. Moraveji et al. [23] modelled fully developed flow in a circular tube with laminar flow, assuming constant heat flux on the tube wall, and using a single phase approach. With nanofluid (up to 6 wt % Al_2O_3 + water), they recorded higher heat transfer than base fluid. Akbari et al. [24] showed, theoretically, the heat transfer improvement with increasing Reynolds number (Re) and concentration of nano-particles in the nanofluid solution (H_2O/Al_2O_3). The two phase model was applied in three different CFD based two phase approaches, i.e. volume of fluid (VOF), mixture and Eulerian. The predictions by the three two-phase models are essentially the same. Therefore, the less expensive model (VOF) is to be preferred for this problem.

Apparently contradicting results in the literature can be related to the method of comparison used. For example some experiments are based on either constant Reynolds number (Re) or constant velocity. Pak and Cho [25] states that the heat transfer is enhanced for turbulent flow of

Al_2O_3-water compared with the basefluid when Re is maintained constant between tests. However, by considering the same value of the velocity for the same case, the heat transfer of the nanofluid reduces. This is because, by adding the nanoparticles to the basefluid the viscosity of the fluid increases, which means the fluid needs more velocity to reach the value of the constant Re, with related heat transfer enhancement by increased turbulence. Yu et al. [26] studied analytically the effects of constant Re, constant velocity and constant power pumping on the heat transfer coefficient improvement, by assuming that the nanofluid obeys a 'classical', single phase, relation of the thermophysical properties. They conclude that the constant pumping power comparison is the most unambiguous; the constant flow velocity comparison can give quite good results under certain conditions but the constant Reynolds number comparison distorts the physical situation, because of changing properties (density and viscosity) of the fluid, and therefore, should not be used.

The characteristics of nano-fluids are seen in the literature to depend on fluid combination, and characteristics of the flow. Modelling is preferred using the two phase approach and with volume of fluid method. In order to establish the characteristics of our fluid, we aim to model a well-established geometrical case with experimental validation and repeat the case with the application of the two phase fluid properties of zinc-bromide-acetone solution with zinc oxide nano-particles.

A flat tube model, simulating part of an automotive heat exchanger provides a good base model for the test. There are several studies dealing with a nanofluid flow in the flat tube [27-33]. Peyghambarzadeh et. al [28] experimentally studied heat transfer in a car radiator using H_2O/EG mixed with different amounts of aluminium oxide Al_2O_3 nanoparticles. They found that the nanofluid enhanced the heat transfer 40% more than the base fluid. Delavari and Hashemabadi [27] presented a CFD model of the heat transfer of the Al_2O_3/H_2O and Al_2O_3/EG nanofluid in the same situation, testing the validity of the single phase and two phase models against experimental results of Peyghambarzadeh et. al [28] concluding that only the two phase model gives good representation of the physical system. They found the Nusselt Number increased by a factor of two by adding 1% Al_2O_3 to water.

In order to provide validation for the numerical simulations, the case of Peyghambarzadeh et. al [28] is numerically repeated to prove the method works in our context. We then apply the same method with our alternative nano-fluid to evaluate its potential for use in a vapour absorption cycle.

2- Geometry and assumptions

The geometrical arrangement in Figure 1, is a flat tube with 31 cm length and 0.53 cm hydraulic diameter.

The system is closed, the nanofluid is incompressible, it is at steady state and under Newtonian flow [27]; evaporation of the acetone is neglected; density of the solution is constant under different pressures; the temperature and inlet velocity is constant; thermal equilibrium is assumed between the base fluid and the nanoparticles; the entering velocities of the fluid and the particles are the same. According to the length of the channel (0.31 m) and the average velocities of the solution (1.5 – 6 m/s) the average time, for the solution to pass through end to end is between (0.05 – 0.2 s).

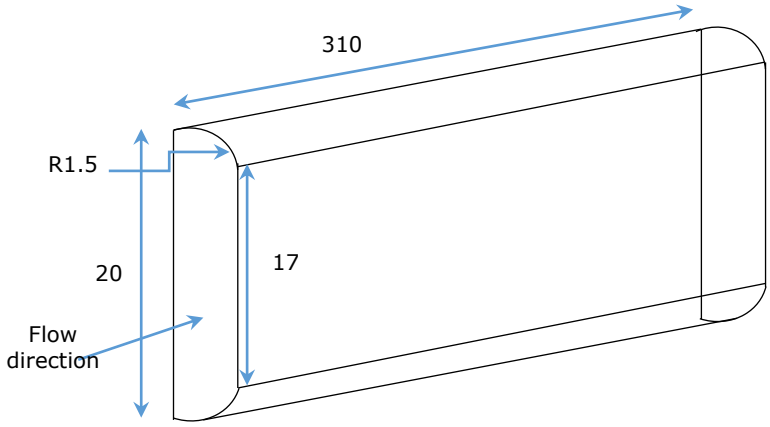

Figure 1. Dimensions of the symmetric flat tube in this study in mm (Not to scale).

3- Nano-fluid properties

The proposed nanofluid ZnO – acetone / $ZnBr_2$ (50 wt. % $ZnBr_2$) was prepared in a laboratory and sonicated with sonication bath (38 KHz) model SW1H produced by NICKEL-ELECTRO LTD in order to demonstrate suspension stability. The samples show stability and good dispersal for 5 hours during a static settling test as illustrated in Figure 2; this time is sufficient to test the fluid in the vapour absorption refrigeration system (VARS). Figure 2 shows the nanofluid with different concentrations of ZnO and different sonication options. For the 0.3 vol. % concentration, the solution converts to brown colour because it was in the ultrasonic bath for 24 hours. The heat generated through the prolonged sonication process converts the solution colour from white to brown. The bottle number 2 was prepared without sonication. The other samples were left in the ultrasonic bath for 2 hrs. The sonication process does not affect the time of sedimentation. In Figure 2-d, by comparing the top part of the bottle 4 with the top part of the bottle 3, it can be seen that the top part of the bottle 4 is clearer than the same region of bottle 3. This is because, bottle 4 contains higher concentration of nanoparticles and the particles are close to each other and the high surface area of the nanoparticles promotes agglomeration and consequently faster sedimentation. However, in bottle number 3 the particles are relatively distant and they need a time to reach to each other and agglomerate. From this behaviour it is concluded that the high concentration nanofluid sediments significantly faster than the dilute nanofluid. Three surfactants were tested with identical nanoparticle concentration suspensions, with addition of 1 wt. % of the surfactants (Poly vinyl pyrrolidone (PVP), Sodium dodecyl sulphate (SDS) and Polyvinyl alcohol (PVA)). These surfactants had no effect on the sedimentation time of nanoparticles in acetone / $ZnBr_2$, separating readily from the base fluid, and the experiments were conducted with no further attempt at suspension enhancement other than the mechanical means described.

4- Two phase CFD methodology

For the two phase model, there are two approaches for simulating: Lagrangian-Eulerian is suitable for the low volumetric concentration and assumes the Eulerian for the continuous fluid (base-fluid) and Lagrangian for the solid particles which are tracked as discrete particles. Eulerian-Eulerian is more suitable for the high volume fraction of the second phase because the calculation of many trajectories for the large dispersion of particles makes the Lagrangian method impractical and non-representative without a large number of particle injections and Lagrangian fails to give a representation of the volume

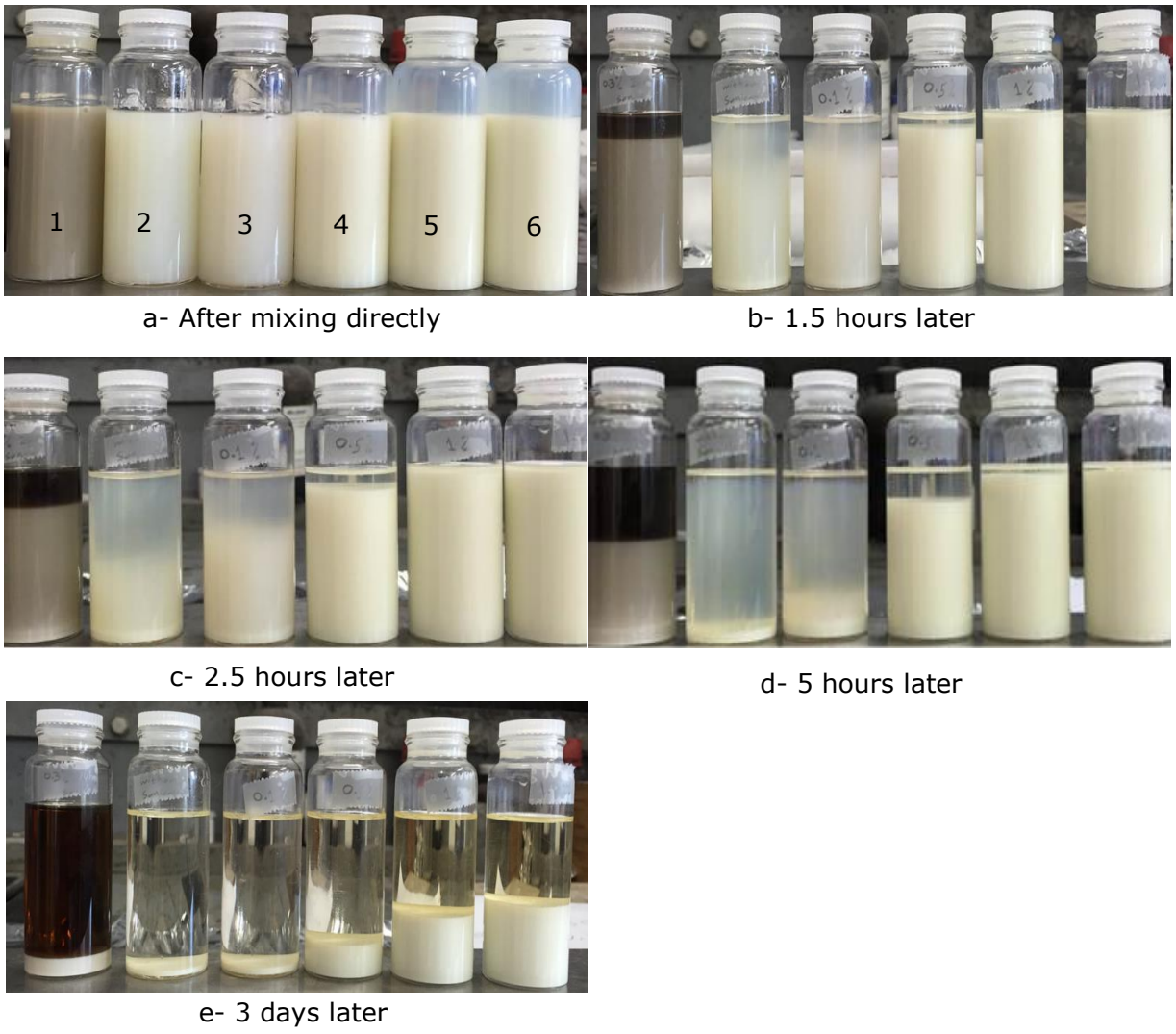

Figure 2. Sedimentation of different concentration of ZnO nanoparticles in Ac.-$ZnBr_2$.
1- 0.3 Vol. % 24 hrs Sonication. 2- 0.005 Vol. %(without sonication). 3- 0.1 Vol. % (2 Hrs Sonication). 4- 0.5 Vol. % (2 Hrs Sonication). 5- 1 Vol. % (2 Hrs Sonication). 6- 1.2 Vol. % (2 Hrs Sonication).

taken by the discrete phase in the continuous phase. This is demonstrated by Delavari and Hashemabadi [27]. The viscous model used in this method is standard k-epsilon model, with enhanced wall treatment. The multiphase model is mixture method and the SIMPLE scheme for the pressure-velocity coupling; the first order upwind method used for all of momentum, volume fraction

and the turbulent kinetic energy and PRESTO method for pressure. The governing equations of the continuity, momentum and energy equations [27, 34] are:

Continuity

$$\nabla.(\rho_m \vec{v}_m) = 0 \quad (1)$$

Momentum

$$(\rho_m \vec{v}_m).\nabla\vec{v}_m = -\nabla P_m + \nabla.(\mu_m \nabla\vec{v}_m) + \rho_m g + \nabla.\sum_{k=1}^{n} \varphi_k \rho_k \vec{v}_{dr,k}\vec{v}_{dr,k} \quad (2)$$

Where

$$\vec{v}_m = \frac{\sum_{k=1}^{n} \varphi_k \rho_k \vec{v}_k}{\rho_m} \quad (3)$$

$$\rho_m = \sum_{k=1}^{n} \varphi_k \rho_k \quad (4)$$

$$\mu_m = \sum_{k=1}^{n} \varphi_k \mu_k \quad (5)$$

$$\vec{v}_{dr,k} = \vec{v}_k - \vec{v}_m \quad (6)$$

Energy

$$\nabla.\sum_{k=1}^{n}\left(\varphi_k \vec{v}_k(\rho_k E_k + P)\right) = \nabla.\left(k_{nf}\nabla T\right) + S_E \quad (7)$$

Where

$$E_k = h_k - \frac{P}{\rho_k} + \frac{v_k^2}{2} \quad (8)$$

Masoumi et al. [35] developed a formula to calculate the viscosity of the particle cloud for the second phase, with respect to the Brownian motion of particles:

$$\frac{\mu_{nf}}{\mu_f} = 1 + \frac{\rho_p v_B d_p^2}{72C\delta} \quad (9)$$

Where v_B (velocity of Brownian motion), δ (the mean distance between the centres of two particles) and C (correction factor) found by equations 10 - 12.

$$v_B = \frac{1}{d_p}\sqrt[3]{\frac{18K_b T}{\pi\rho_p d_p}} \quad (10)$$

$$\delta = \sqrt[3]{\frac{\pi d_p}{6\varphi}} \qquad 11$$

$$C = \frac{a\Omega + b}{\mu_f} \qquad 12$$

Where K_b is Boltzmann constant (1.38 x 10^{-23} m^2kg/s^2K), a=-4 x 10^{-5} and b=7.13 x 10^{-7} and it is found to be valid only when $\Omega < -b/a$. For the two phase model the software calculates the properties of the nanofluid implicitly for varying concentration of nano-particles according to equations 4 and 5.

The viscosity of the nanoparticles cloud is calculated by equation 9 together with the viscosity of the combination of the base fluid alone and of the cloud of nanoparticles as expressed in equation 5. This technique to find the viscosity of the cloud of nanoparticles in the fluid as used by [35], however [27, 28] are used a different strategy to find the viscosity of the nanoparticles using trial and error; the viscosity of the nanoparticles was varied until the pressure drop and Nusselt number of the very dilute nanofluid, pure ethylene glycol at Re=2440, and pure water at Re=9350, were equal. We confirm that the methods are equivalent in effect.

5- Boundary condition for the novel refrigerant simulation

Initially a validation exercise was conducted, repeating the method of Delavari and Hashemabadi to prove correct application of the method, and following this the numerical calculation was done with laminar and turbulent flow conditions for the proposed nanofluid depending on the mass concentration of acetone. To keep the velocity of the fluid comparable to that used in the literature ([27, 28]), Reynolds number was taken in four ranges as shown in Table 1.

Table 1. Reynold number at a different mass fraction of acetone.

Ac. Mass fraction	30%	40%	50%	60%	70%
Re	150-300	1500-3000	5000-10000	15000-25000	15000-25000

The temperature of the inlet flowing nanofluid is 323 K, the turbulence intensity is in the order of 10%, depending on a calculated value, and the hydraulic diameter is 0.53 cm. A convection boundary condition was assumed for the wall from outside with the heat transfer coefficient at the wall specified as 150 W/m^2K and the external air temperature as 303 K.

6- Results and discussion

6.1- Justification of mesh structure

The commercial code Ansys® Fluent is used to simulate this flow situation using the Eulerian-Eulerian method (mixture model). Four mesh sizes were selected in order to achieve a minimum

number of cells with accurate results. The meshes were compared by the heat transfer coefficient on the wall using 50 wt. % acetone/zinc bromide with a turbulent flow (Re=8000). The results shown in table 2 were very similar especially for meshes (2, 3 and 4) but because meshes 3 & 4 have more nodes, and therefore lengthier simulation, the best mesh regarding accuracy and time was mesh 2 as shown in Figure 3. The computer used has processer 3.7 GHz (Intel® Xeon® CPU E5—1620 v2 @ 3.7GHz) with the memory (RAM) 32 GB.

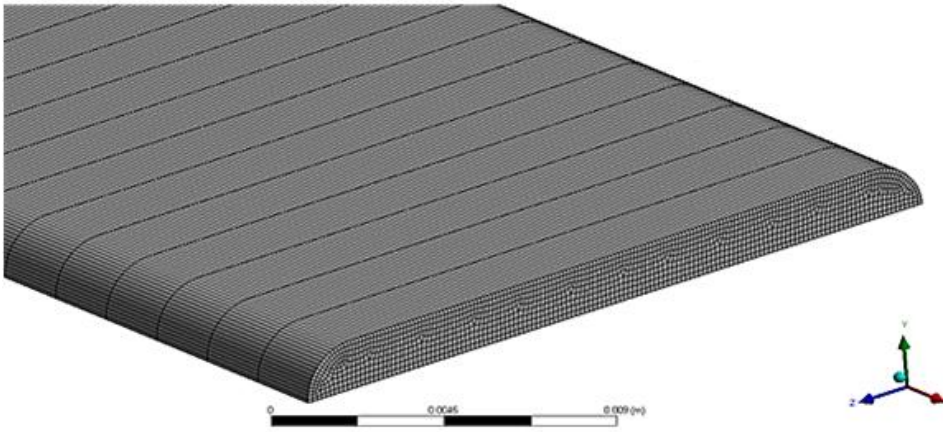

Figure 3. Mesh #2 used in this study.

Table 2**.** Mesh independence study of the fully developed region using 50wt. % Ac./$ZnBr_2$ with Re=8000.

#	Mesh (x, z, y)	Heat trans. Coff. (W/K. m^2)	Clock time for simulation (min)
1	130 x 130 x 15	3150.01	12
2	140 x 140 x 20	3151.916	14
3	150 x 150 x 20	3151.927	18
4	180 x 160 x 22	3151.933	25

6.2- Validation of the CFD Modelling

To validate the accuracy of this model, the experimental data of the heat transfer improvement using water based nanofluid (Al_2O_3 / H_2O) as a coolant in a car radiator which presented by Peyghambarzadeh et al. [28] was compared to corresponding the current numerical results. Peyghambarzadeh et al. conducted uncertainty analysis for their experiments depending on the single sample uncertainty zeroth order (defining as fixed and random errors presented just by the instrumentation, with no contribution from the process) analysis method for each measurement, which is described by Moffat [36]. They state that the uncertainty of the Nu (18% 24<Nu<120) caused by the error Re (5.5% 1200<Re<23000) and the measured temperature. Furthermore, they compared their experimental Nu with the correlation of Xuan and Li [37] and they found a good agreement presented by 7% (vertical bar) error for the nanofluid Al_2O_3 / H_2O as shown in figure (4). The figure also shows how the 18% error of the measured Nu appears on the graph as the horizontal bar.

The validation of the simulation work with an experimental work has been done previously in many studies, such as the validations in [27, 38]. In our work, the same geometry of Peyghambarzadeh et al [28] is built in Ansys® Fluent and the same boundary conditions and properties of the nanofluid are applied on the numerical model (using the method described above) as in the physical experiment. The results of enhancement of Nusselt number as a function of the volume fraction, and of Nusselt number as a function of the flow rate show an acceptable agreement with the previous experimental work as shown in Figure 5.

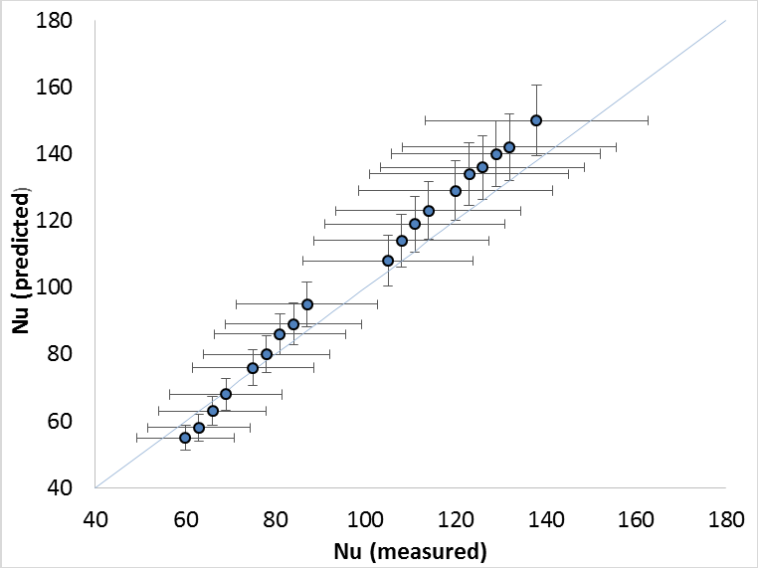

Figure 4. Comparison between the experimental Nu from [28] and the predicted Nu from [37]. Horizontal error bars are experimental uncertainty (18%) [28]; vertical error bars are error of analytical prediction (7%) [37]. This figure is reproduced by permission from [28].

Figure 5a shows the relation of enhancement of Nu with nano-particle concentration at Re of 13800 and 23000 and inlet temperature of 308 K. It shows at most a 4 % discrepancy between the experimental and the numerical work. Figure 5b shows Nu as a function of flow rate at the nanoparticle volume fraction of 1 % in both experimental (previous work) and CFD (current work), with maximum difference between the experiment and numerical results of 9 %. The difference could be caused by some factors such as particle size, which effect on the viscosity, temperature dependant properties and the Brownian motion of the particles which effect on the thermal conductivity [38-40].

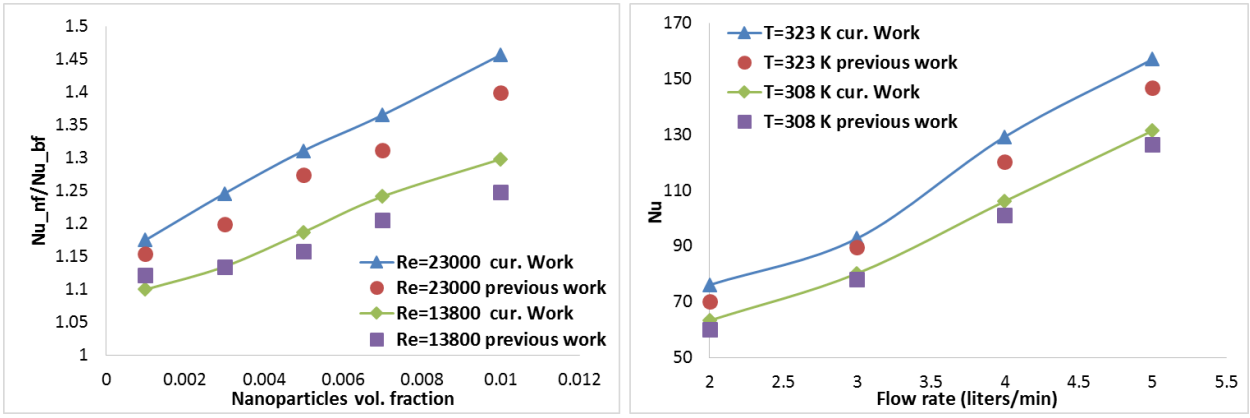

a b

Figure 5. Comparison between a- enhancement in the Nusselt number as a function of a nanoparticle volume fraction in water at 308 K and B- Nusselt number as a function of a flow rate at the nanoparticles volume concentration of 1 % of both the simulation work and the experimental work of [28].

6.3- Effects on the centreline velocity

To understand the behaviour of the velocity development along the tube and how the parameters affected it, a centreline velocity is analysed under the effects of the variation of the concentrations of both acetone and nanoparticles. This provides a reasonable representation of the variation of flow dynamics between the various cases. Centreline velocity is usually a maximum velocity in the pipe and it is greater than the average velocity. For example, for a laminar circular pipe flow, the maximum (centreline) velocity is equal to double the mean velocity and in the rectangular duct the maximum velocity is 1.5 of the average velocity [8]. According to the data collected from different cases in the present work the maximum velocities in the laminar and turbulent flow for all cases with all concentrations:

$V_{cl} = 1.4 * V_{av}$ Laminar

$V_{cl} = 1.15 * V_{av}$ Turbulent

The centreline velocity has a development length and settles to a final constant value (Figure 6). The centreline velocity decreases slightly by increasing the concentration of the nanoparticles as shown in Figure 7 due to increasing density of the nanofluid. Increasing acetone decreases the density, but the viscosity drops significantly, for example, it drops from 1.29 mPa.s to 0.63 mPa.s [2], when the mass fraction of acetone increases from 60wt. % to 70wt. % and the shape of the centreline velocity profile is correspondingly more uniform along the length (Figure 6). Thus although decreasing density implies high velocity, the viscosity increase flattens the velocity profile.

6.4- Effects on the wall shear stress and skin friction

The average Y plus (y^+) at the tube wall (for the case Re=8000, acetone concentration =50 wt. % & nanoparticles concentration= 0.5 vol. %) was measured. Enhanced wall treatment was implemented in the turbulent flow simulation, which should produce a y+ value equal to one. The average y^+ at the tube wall is 8.1 for the curve edge of the wall (semi-circular wall) and 0.98 for the flat wall. The good agreement with the existing results, shows that the application of the method in our case is reliably repeated.

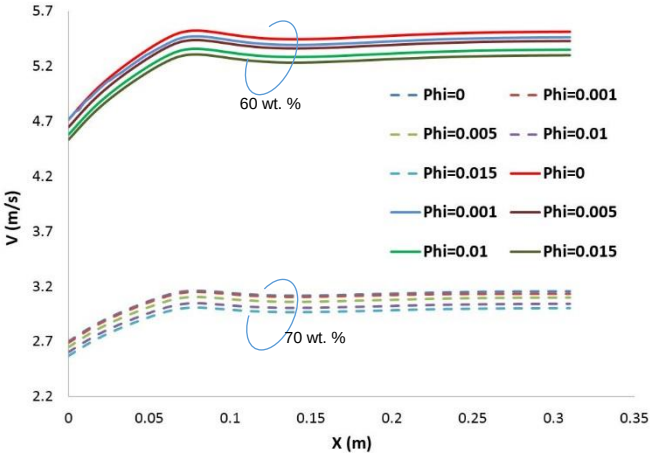

Figure 6. Centreline velocity along the tube with different concentration of ZnO nanoparticles and 60% & 70% of acetone at Re of 25000.

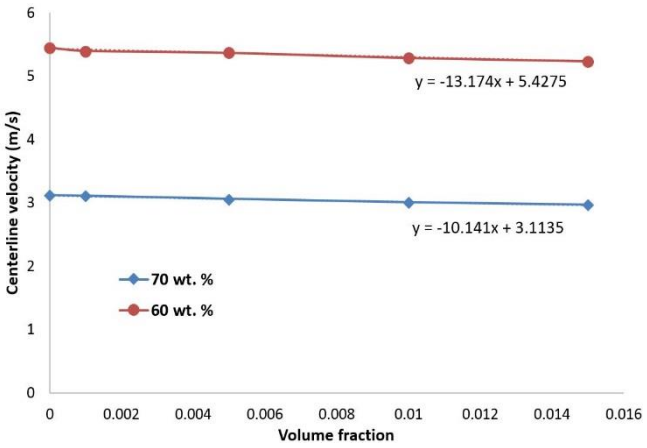

Figure 8. Centreline velocities as function of volume fraction at distance 0.15m from the inlet of the tube for the both cases 60wt. % and 70wt. %.

The magnitude of the wall shear stress, $\tau_w = \mu\left(\frac{du}{dy}\right)$ and the skin friction coefficient $C_f = \frac{\tau_w}{0.5\rho v^2}$ describe the heat transfer by virtue of the Reynolds analogy, $h = \frac{C_f}{2}$.

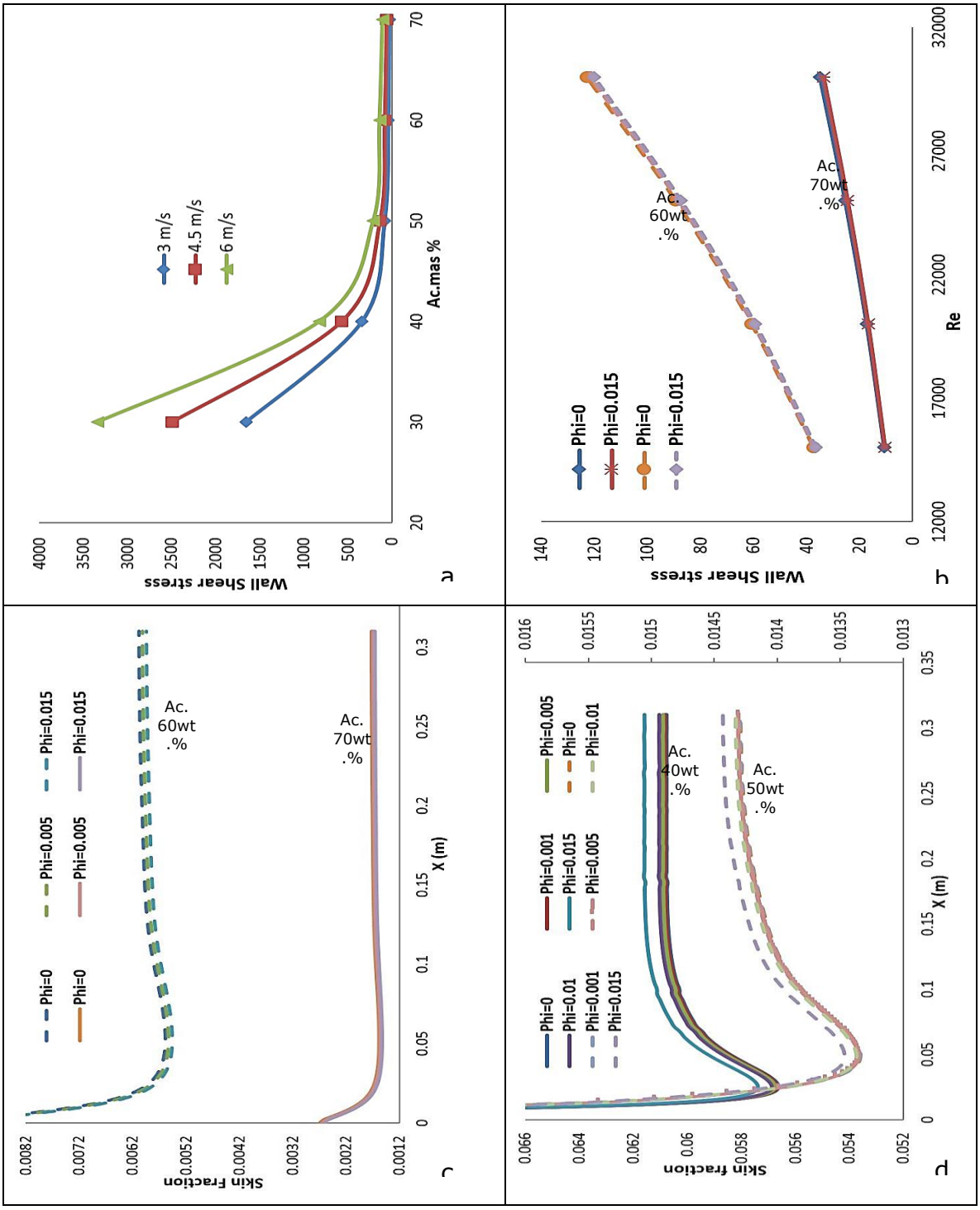

Figure 7. a) wall shear stress and the acetone concentration at different velocity and 0.01 volume fractions of nanoparticles; b) wall shear stress and Re different concentration of ZnO nanoparticles and 60% & 70% of acetone; c) skin friction with different concentration of a nanoparticles at Re=20000 and for Ac. 60wt. % and 70wt. %; d) skin friction with different concentration of nanoparticles for Ac. 40wt. % with Re=2500 and 50wt. % with Re of 12000.

The effect of the acetone mass fraction on the wall shear stress is illustrated in Figure 8a and Figure 7b shows variation with Re. Figure 8b shows that the effect of the nanoparticles concentration is indiscernible on the wall shear stress. Acetone concentration has a significant effect due to viscosity, especially below 40% concentration.

Figure 8c shows that the skin friction decreases with increasing acetone mass fraction. It also illustrates that the skin friction decreases slightly with increasing the volume fraction of nanoparticles. This will change with reducing the acetone concentration and the Reynolds number to less than 60% and 15000 respectively, in this range the skin friction increases with increasing volume fraction of ZnO (Figure 8d). This result partially contradicts the result of Delavari and Hashemabadi [27] who state that the skin friction only increases as the nanoparticles volume fraction increases. For a high Re (low viscosity, e.g. 60-70 wt. % acetone) particles cause a lower skin friction; this may be explained by decreased interaction of particles, which are carried by the convective stream of fluid, in the steep velocity gradient boundary layer. However, for the low Re (high viscosity) like water in Delavari and Hashemabadi study [27] and for the 40 - 50 wt. % acetone case, the behaviour of the particles near to the surface may be different due to the less steep velocity gradient giving more time for particle interaction.

6.5- Effect on the heat transfer coefficient

Figure 9a shows that the heat transfer increases with Reynolds number, as expected. Figure 9b shows the enhancement of average heat transfer coefficient related to the concentration of nanoparticles: for acetone mass fraction 50% the enhancement of the heat transfer coefficient can reach 180% of the original base fluid value and this type of behaviour is confirmed by previous studies [24, 27, 41].

As shown in Figure 9c the heat transfer coefficient increases with acetone fraction and velocity for 1% nanoparticle volume concentration; with a low concentration of acetone (for example 30 wt. %) the density and the viscosity of the fluid are very high (2617 kg/m^3 and 263.3 mPa.s [2]), nanofluid motion is restricted and the heat transfer is poor, especially for low temperature conditions. The Nusselt number increases with particle volume fraction and the Nusselt number of the C_3H_6O (acetone)/ZnO for acetone greater than 50% by mass, is greater than that of the H_2O/Al_2O_3 used by [27] for the same volume fraction and Re as shown in Figure 9d.

Table shows numerical results for the heat transfer coefficient with varying concentrations of acetone, nanoparticles and Reynolds number. The nanofluid density, viscosity and thermal conductivity increase and the specific heat decreases with addition of only a small volume of nanoparticles; the heat transfer of the nanofluid is significantly affected as indicated in the table. The nano-particle influence in particular can be explained by the Brownian motion effect on viscosity indicated by equation 9. The boundary layer thickness decreases because of the random motion of nanoparticles in the fluid and this leads to increasing the heat transfer between the wall and the bulk fluid [29].

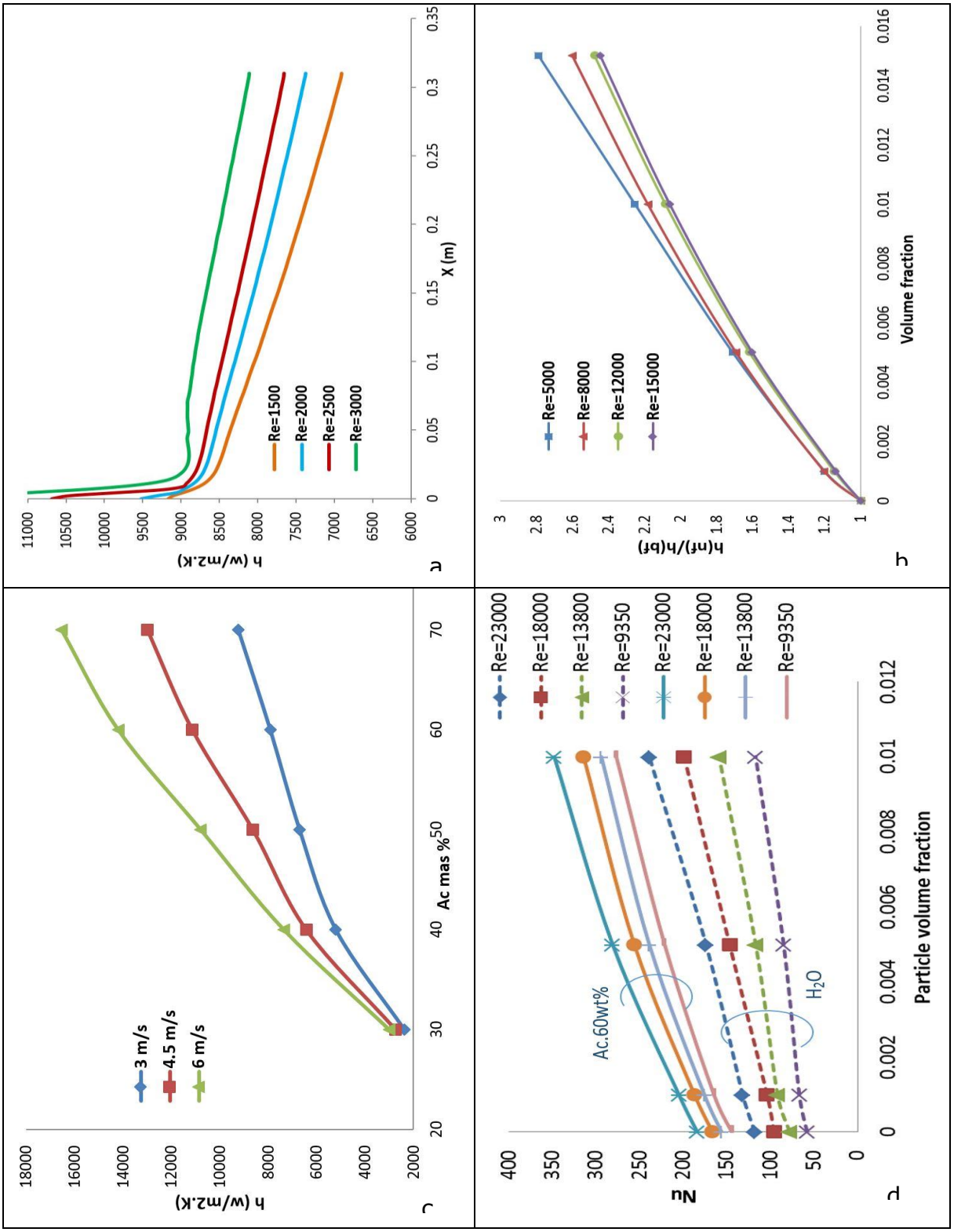

Figure 8. a) Variation of the heat transfer coefficient along the tube wall in both of single and two phase approaches for the same values of Re. b) Variations of the numerical results of h_{nf}/h_{bf} with different concentration of nanoparticles in two phase approach. c) Relation between heat transfer coefficient and acetone mass fraction with different velocity of fluid and volume fraction of nanoparticles of 0.01. d) Nusselt number as function of the volume fraction for different Re and for H_2O/Al_2O_3 which used by [23] and acetone zinc bromide (Ac. 60%)/ ZnO for a two phase model flow.

Table 4. Numerical results of the heat transfer coefficient with different concentration of acetone and nanoparticles and different Re.

Ac. Mass fraction	Re	0%	0.1%	0.5%	1%	1.5%
		h ($W/m^2.K$)				
30%	200	1158	1360	1942	2559	3106
	250	1231	1463	2095	2763	3357
	300	1289	1550	2227	2942	3576
40%	2000	2641	3009	4356	6243	8013
	2500	3017	3415	4860	6483	8281
	3000	3384	3823	5372	7090	8657
50%	8000	3336	3792	5330	6874	8192
	12000	4290	4877	6875	8856	10526
	15000	5150	5856	8239	10599	12580
60%	20000	4786	5420	7458	9343	10841
	25000	5799	6575	9016	11286	13074
	30000	6788	7672	10536	13163	15229
70%	20000	3636	4106	5554	6809	7754
	25000	4400	4967	6702	8196	9318
	30000	5145	5804	7817	9545	10835

7- Conclusion

Laminar and turbulent mixed convection of acetone/$ZnBr_2$-ZnO nanofluid inside a flat tube were studied numerically using a two phase mixture approach. The validation of this work was confirmed by repeating a case for a nanofluid (Al_2O_3-H_2O) which was used by the experimental work of Peyghambarzadeh [28] and a good agreement was found, demonstrating reliable implementation of the method. The main part of the study goes on to show that for the acetone-zinc bromide solution with ZnO nano-particles, the heat transfer increases with Re and concentration of both nanoparticles and acetone, as expected from the literature. The two phase method shows a strong effect of the nanoparticles on improving the heat transfer, which given the reliability of the method in the previous case of [27], provides reasonable confidence in a positive outcome in the event of using the fluid in a heat transfer situation like the absorption refrigeration cycle.

Wall shear stress increases with increasing Re and decreases with increasing acetone concentration because the viscosity of the fluid decreases; it is not altered noticeably by changing the concentration of nanoparticles. Increased wall shear stress indicates improved heat transfer to the wall, therefore there is not a direct heat transfer benefit due to nano particles by the wall shear stress. The behaviour of the skin friction depends on the concentration of acetone as well as Re as reflected in the wall stress. The effect of increasing concentration of nano-particles on the skin friction is significantly affected by acetone concentration and Re: the skin friction decreases with increasing concentration of nanoparticles at 70wt. % of acetone and Re of 20000, but it

increases with increasing volume fraction of the nanoparticles at 60wt. % of acetone and Re of 15000. We suggest that this may be due to particle interaction increasing in the low Re velocity gradient, where there is increased interaction time as suggested in the formulation of nano-particle cloud viscosity used. The overall performance of the solution with the nano-particles shows a promising enhancement for the heat transfer challenge of the vapour absorption refrigeration system, since an enhancement of up to 180% of basefluid can be achieved with only 1.5% volume fraction of particles. The concentration of the salt solution base fluid is a significant effector of heat transfer enhancement together with the nano-particles.

References

[1. Sun, J., L. Fu, and S. Zhang, *A review of working fluids of absorption cycles.* Renewable and Sustainable Energy Reviews, 2012. **16**(4): p. 1899-1906.
2. Ajib, S. and A. Karno, *Thermo physical properties of acetone–zinc bromide for using in a low temperature driven absorption refrigeration machine.* Heat and Mass Transfer, 2008. **45**(1): p. 61-70.
3. Han, Z., *Nanofluids with enhanced thermal transport properties*. 2008. p. 2.
4. Wen, D. and Y. Ding, *Formulation of nanofluids for natural convective heat transfer applications.* International Journal of Heat and Fluid Flow, 2005. **26**(6): p. 855-864.
5. Hwang, K.S., S.P. Jang, and S.U.S. Choi, *Flow and convective heat transfer characteristics of water-based Al2O3 nanofluids in fully developed laminar flow regime.* International Journal of Heat and Mass Transfer, 2009. **52**(1–2): p. 193-199.
6. Wen, D. and Y. Ding, *Experimental investigation into convective heat transfer of nanofluids at the entrance region under laminar flow conditions.* International Journal of Heat and Mass Transfer, 2004. **47**(24): p. 5181-5188.
7. Ding, Y., et al., *Heat transfer of aqueous suspensions of carbon nanotubes (CNT nanofluids).* International Journal of Heat and Mass Transfer, 2006. **49**(1–2): p. 240-250.
8. Garg, P., et al., *An experimental study on the effect of ultrasonication on viscosity and heat transfer performance of multi-wall carbon nanotube-based aqueous nanofluids.* International Journal of Heat and Mass Transfer, 2009. **52**(21–22): p. 5090-5101.
9. Liao, L. and Z.-H. Liu, *Forced convective flow drag and heat transfer characteristics of carbon nanotube suspensions in a horizontal small tube.* Heat and Mass Transfer, 2009. **45**(8): p. 1129-1136.
10. Takabi, B., A.M. Gheitaghy, and P. Tazraei, *Hybrid Water-Based Suspension of Al2O3 and Cu Nanoparticles on Laminar Convection Effectiveness.* Journal of Thermophysics and Heat Transfer, 2016. **30**(3): p. 523-532.
11. Takabi, B. and H. Shokouhmand, *Effects of Al2O3–Cu/water hybrid nanofluid on heat transfer and flow characteristics in turbulent regime.* International Journal of Modern Physics C, 2015. **26**(04): p. 1550047.
12. Sarkar, J., P. Ghosh, and A. Adil, *A review on hybrid nanofluids: recent research, development and applications.* Renewable and Sustainable Energy Reviews, 2015. **43**: p. 164-177.
13. Timofeeva, E.V., J.L. Routbort, and D. Singh, *Particle shape effects on thermophysical properties of alumina nanofluids.* Journal of Applied Physics, 2009. **106**(1): p. 014304.
14. Timofeeva, E.V., et al., *Base fluid and temperature effects on the heat transfer characteristics of SiC in ethylene glycol/H2O and H2O nanofluids.* Journal of Applied Physics, 2011. **109**(1): p. 014914.
15. Williams, W., J. Buongiorno, and L.-W. Hu, *Experimental Investigation of Turbulent Convective Heat Transfer and Pressure Loss of Alumina/Water and*

Zirconia/Water Nanoparticle Colloids (Nanofluids) in Horizontal Tubes. Journal of Heat Transfer, 2008. **130**(4): p. 042412-042412.
16. Utomo, A.T., et al., *The effect of nanoparticles on laminar heat transfer in a horizontal tube.* International Journal of Heat and Mass Transfer, 2014. **69**: p. 77-91.
17. Rea, U., et al., *Laminar convective heat transfer and viscous pressure loss of alumina–water and zirconia–water nanofluids.* International Journal of Heat and Mass Transfer, 2009. **52**(7–8): p. 2042-2048.
18. Pantzali, M.N., et al., *Effect of nanofluids on the performance of a miniature plate heat exchanger with modulated surface.* International Journal of Heat and Fluid Flow, 2009. **30**(4): p. 691-699.
19. Jafari, A., M.H. Rahimian, and A. Saeedmanesh, *An unsteady mixed convection in a driven cavity filled with nanofluids using an externally oscillating lid.* Journal of Electronics Cooling and Thermal Control, 2013. **3**(2): p. 58.
20. Demir, H., et al., *Numerical investigation on the single phase forced convection heat transfer characteristics of TiO2 nanofluids in a double-tube counter flow heat exchanger.* International Communications in Heat and Mass Transfer, 2011. **38**(2): p. 218-228.
21. Sinan;, G., A. Kunt;, and E. Hakan, *Comparison of single and two-phase models for nanofluid convection at the entrance of a uniformly heated tube.* International Journal of Thermal Sciences, 2014. **80**(1): p. 83-92.
22. Amoura, M., et al., *Study of Heat Transfer of Nanofluids in a Circular Tube.* International Journal of Mathematical, Computational, Statistical, Natural and Physical Engineering, 2013. **7**(9): p. 6.
23. Moraveji, M.K., et al., *Modeling of convective heat transfer of a nanofluid in the developing region of tube flow with computational fluid dynamics.* International Communications in Heat and Mass Transfer, 2011. **38**(9): p. 1291-1295.
24. Akbari, M., N. Galanis, and A. Behzadmehr, *Comparative analysis of single and two-phase models for CFD studies of nanofluid heat transfer.* International Journal of Thermal Sciences, 2011. **50**(8): p. 1343-1354.
25. Pak, B.C. and Y.I. Cho, *HYDRODYNAMIC AND HEAT TRANSFER STUDY OF DISPERSED FLUIDS WITH SUBMICRON METALLIC OXIDE PARTICLES.* Experimental Heat Transfer, 1998. **11**(2): p. 151-170.
26. Yu, W., et al., *Thermophysical property-related comparison criteria for nanofluid heat transfer enhancement in turbulent flow.* Applied Physics Letters, 2010. **96**(21): p. 213109.
27. Delavari, V. and S.H. Hashemabadi, *CFD simulation of heat transfer enhancement of Al2O3/water and Al2O3/ethylene glycol nanofluids in a car radiator.* Applied Thermal Engineering, 2014. **73**(1): p. 380-390.
28. Peyghambarzadeh, S., et al., *Experimental study of heat transfer enhancement using water/ethylene glycol based nanofluids as a new coolant for car radiators.* International Communications in Heat and Mass Transfer, 2011. **38**(9): p. 1283-1290.
29. Peyghambarzadeh, S.M., et al., *Experimental study of overall heat transfer coefficient in the application of dilute nanofluids in the car radiator.* Applied Thermal Engineering, 2013. **52**(1): p. 8-16.
30. Safikhani, H. and A. Abbassi, *A new dispersion model for thermal properties of nanofluids in flat tubes.* International Journal of Thermal Sciences, 2016. **109**: p. 114-122.
31. Vajjha, R.S., D.K. Das, and P.K. Namburu, *Numerical study of fluid dynamic and heat transfer performance of Al2O3 and CuO nanofluids in the flat tubes of a radiator.* International Journal of Heat and Fluid Flow, 2010. **31**(4): p. 613-621.
32. Vajjha, R.S., D.K. Das, and D.R. Ray, *Development of new correlations for the Nusselt number and the friction factor under turbulent flow of nanofluids in flat tubes.* International Journal of Heat and Mass Transfer, 2015. **80**: p. 353-367.
33. Zhao, N., et al., *Numerical investigations of laminar heat transfer and flow performance of Al2O3–water nanofluids in a flat tube.* International Journal of Heat and Mass Transfer, 2016. **92**: p. 268-282.

34. *Fluent 15 User's Guide*. 2015.
35. Masoumi, N., N. Sohrabi, and A. Behzadmehr, *A new model for calculating the effective viscosity of nanofluids.* Journal of Physics D: Applied Physics, 2009. **42**(5): p. 055501.
36. Moffat, R.J., *Describing the uncertainties in experimental results.* Experimental thermal and fluid science, 1988. **1**(1): p. 3-17.
37. Xuan, Y. and Q. Li, *Investigation on convective heat transfer and flow features of nanofluids.* Journal of Heat transfer, 2003. **125**(1): p. 151-155.
38. Helvaci, H. and Z.A. Khan, *Heat transfer and entropy generation analysis of HFE 7000 based nanorefrigerants.* International Journal of Heat and Mass Transfer, 2017. **104**: p. 318-327.
39. Bianco, V., et al., *Numerical investigation of nanofluids forced convection in circular tubes.* Applied Thermal Engineering, 2009. **29**(17): p. 3632-3642.
40. Xuan, Y. and Q. Li, *Heat transfer enhancement of nanofluids.* International Journal of heat and fluid flow, 2000. **21**(1): p. 58-64.
41. Kalteh, M., et al., *Eulerian–Eulerian two-phase numerical simulation of nanofluid laminar forced convection in a microchannel.* International Journal of Heat and Fluid Flow, 2011. **32**(1): p. 107-116.